Journal of Alloys and Compounds 505 (2010) 717–721

Contents lists available at ScienceDirect

Journal of Alloys and Compounds

journal homepage: www.elsevier.com/locate/jallcom

Feasibility study of the direct synthesis of $Mg(BH_4)_2$ complex hydrides by mechanical milling

Z.G. Zhang, S.F. Zhang, H. Wang, J.W. Liu, M. Zhu*

School of Materials Science and Engineering, South China University of Technology, 510640 Guangzhou, PR China

ARTICLE INFO

Article history:
Received 13 April 2010
Received in revised form 15 June 2010
Accepted 16 June 2010
Available online 30 June 2010

Keywords:
Mg(BH4)2
Ball milling
Hydrogen storage
Grain size
Particle size

ABSTRACT

Magnesium borohydride [$Mg(BH_4)_2$] is a promising complex hydride for hydrogen storage. This study reports a feasibility study of the synthesis of $Mg(BH_4)_2$ by planetary ball milling of pure Mg–B powder and then a hydrogenation process under a hydrogen atmosphere. The ball milling parameters were firstly optimized. The Mg–B powders with the smallest average particle size of 1.91 ± 1.61 μm and the smallest average crystallite size of 9.4 ± 1.1 nm were used. However, no successful synthesis of $Mg(BH_4)_2$ was achieved. The obtained nanocrystalline hydride was MgH_2. It was found that the addition of B into magnesium strongly enhanced the kinetic properties of magnesium hydrogenation. The reduction of crystallite size showed a more obvious effect on improving the absorption kinetic properties than that of the particle size. The powder of the smallest crystallite size after hydrogenation comprised a minute amount of B–H compounds. The formation of $Mg(BH_4)_2$ from pure elements was difficult because of the barriers against breaking the B–B atomic bonds and the migration of the B atoms.

1. Introduction

A crucial issue for the application of hydrogen in fuel cell vehicles is the development of available on-board hydrogen storage systems and materials [1–3]. Low weight complex hydrides such as alanates $[AlH_4]^-$, amides $[NH_2]^-$ and borohydrides $[BH_4]^-$ that combine high volumetric and gravimetric hydrogen densities are the most promising hydrogen storage candidates to fulfill the capacity requirements among all the hydrogen storage materials [4–6].

Magnesium borohydride [$Mg(BH_4)_2$] is a promising complex hydride for hydrogen storage. It possesses not only high gravimetric (14.8 wt.%) and volumetric (112 g/l) hydrogen densities but also a low hydrogen binding enthalpy [7–9]. Moreover, research results concerning the correlation between the thermodynamic stability of $M(BH_4)_n$ (M = Li, Na, K, Ca, Mg, Zn Sc, Zr and Hf; $n = 1–4$) and the electronegativity of M suggest that $Mg(BH_4)_2$ is one of the most attractive candidates for hydrogen storage material owing to its favorable desorption hydrogen enthalpy [8,10]. However, because of the kinetic limitations, the lack of reversibility of $Mg(BH_4)_2$ represents a yet unsolved problem. The high decomposition temperature of about 300 °C makes it unfavorable in practical fuel cell application [11,12]. In addition, although a series of theory research has been carried out, the accurate structure and physical properties of $Mg(BH_4)_2$ remain unclear because of the complicated structure arrangements and the difficulty in preparing pure $Mg(BH_4)_2$ [7,11,13–16].

The research results of Vajeeston et al. reveal that from a thermodynamic view the preparation of $Mg(BH_4)_2$ from pure magnesium and boron elements is the better route than starting from the binary hydrides [13]. However, such a direct synthesis method might differ when reaction kinetics is taken into account. The high reaction activation energy of $Mg(BH_4)_2$ is one of the barriers to improving its hydrogen sorption kinetic. Fortunately, the barrier can be tailored by reducing the crystallite size, especially to a nanometer range [12].

Mechanical milling has been widely used to obtain nano-scale hydrides and disperse catalysts into chemical hydrides, thereby generating nanosized catalysts [2,17,18]. The obtained nanostructured materials by ball milling have large surface areas, which facilitate the forming of defects on the particle surface, shortening of the diffusion length of constitutive elements and lowering of hydrogen reaction enthalpy [12]. In this study, the exploration of feasibility to synthesize $Mg(BH_4)_2$ directly from pure magnesium and boron elements using a ball milling method will be carried out since the other chemical synthesis methods present other disadvantages [15]. The synthesis of the Mg–B powder hydrogen storage properties and feasibility of this method will be discussed.

2. Experimental details

The mechanical milling process was performed using a planetary ball milling machine (*QM-3SP2*, Nanjing, China) at room temperature. Commercially available

* Corresponding author. Tel.: +86 20 8711 1216; fax: +86 20 8711 1317.
E-mail address: memzhu@scut.edu.cn (M. Zhu).

0925-8388/$ – see front matter © 2010 Elsevier B.V. All rights reserved.
doi:10.1016/j.jallcom.2010.06.123

Table 1
Assignment of factors and levels of $L_9(3^4)$ orthogonal array.

Factors Levels	A Weight ratio of ball to powder	B Weight ratio of big balls to small balls *D* (10 mm):*D* (6 mm)	C Working time versus rest time (min)	D Milling speed (RPM)
1	10:1	30%:70%	30:30	300
2	20:1	50%:50%	40:20	400
3	15:1	70%:30%	60:30	500

Table 2
$L_9(3^4)$ orthogonal array matrix and crystallite size and particle size.

Experimental series	A	B	C	D	Crystallite size of Mg (nm)	Particle size (μm)
0	Mixture of pure Mg and B				24.1(2.2)	75.1
1	1	1	1	1	28.4(2.2)	1.91(1.62)
2	1	2	2	2	21.6(2.5)	2.59(2.29)
3	1	3	3	3	9.3(1.7)	2.55(2.95)
4	2	1	2	3	13.2(1.5)	3.20(2.64)
5	2	2	3	1	29.3(3.4)	3.62(5.14)
6	2	3	1	2	18.1(6.6)	3.79(4.76)
7	3	1	3	2	9.4(1.1)	3.80(5.63)
8	3	2	1	3	5.4(2.3)	4.83(6.17)
9	3	3	2	1	19.5(1.5)	3.49(3.92)

Mg powder with a purity of 99.9% and amorphous B powder with a purity of 99% were mixed as the raw milling materials. The mixed powder with a mole ratio of Mg:B = 1:2 (Mg: 2.4 g; B: 2.2 g) was sealed in a cylindrical stainless steel vial of 250 ml. The vials were then loaded with two types of stainless steel balls (*D* = 10 mm and *D* = 6 mm). The loading and unloading operations were always handled in a glove box filled with purified argon gas. The dry milling process was carried out in an interval milling mode under an argon protective atmosphere to avoid elevated temperature and oxidation. The total working time of the mill machine was fixed to 12 h. To minimize the particle size and crystallite size, an orthogonal array was designed to optimize the milling parameters. The weight ratio of ball to powder, weight ratio of big balls to small balls (*D* (10 mm):*D* (6 mm)), working time versus cooling time (min) and milling speed were selected as the factors. The details of the orthogonal array are shown in Tables 1 and 2.

Particle size measurement was carried out by attaching the milled powder to a sticky carbon tape and taking pictures under a scanning electron microscope (SEM) (Nova nano SEM430). The obtained images were then analyzed using the ImageJ software. The average particle size was determined as the particle equivalent circle diameter. X-ray diffraction (XRD) analysis was performed on a Philips X-Pert diffractometer with Cu Ka radiation (λ = 0.15406 nm). To avoid exposure to air, the samples were filled into a glass sample holder in an argon glove box and sealed with 3 M Scotch tape. The average crystallite size of Mg powder was calculated from the broadening of the Mg diffraction peaks by taking into account the contribution of the grain refinement and lattice strain [19]. The hydriding reactions of the milled Mg–B powder were conducted using a Sieverts apparatus (AMC gas reaction controller, USA). The Raman spectra of the samples were recorded using a LabRAM Aramis spectrometer excited by a 532 nm laser. Transmission electron microscopy (TEM; JEM-2100, 200 kV) was used to observe the particle morphology, element distribution and phase compositions by dispersing some powder on a microgrid mesh.

3. Experimental results

3.1. Ball milling parameter optimization of Mg–B powder

Fig. 1 shows the XRD patterns of the milled powders in different experiment numbers and the unmilled mixture of the Mg–B powder. The X-ray pattern of the unmilled mixed powders demonstrates the coexistence of a hexagonal phase of magnesium and magnesium hydroxide. The latter is probably from the impurity of the magnesium powder or the slow deliquescence during a long-term reservation. No diffraction peaks, even the amorphous halo from the amorphous boron, can be observed. The amorphous halo tail at the low angle came from the covered Scotch tape. There is no substantial change in the milled Mg–B powder compared with the unmilled powder. The occurrence of a peak at 44.7° can be attributed to the deciduous steel since an intensive Fe signal can be detected in the Energy Dispersive X-ray (EDX) measurements. After the ball milling, some of the diffraction peaks of the Mg phase are broadened, which indicated the variations of the crystallite size at different experiment conditions. However, no shift (or even a very small shift) of the diffraction peaks can be found for all the Mg peaks. From the XRD patterns, it can be concluded that no other phase such as the solid solution of Mg or MgB_2 phase was formed during the milling process. This is different from the results reported by Wronski et al., who demonstrated that a MgB_2 phase formed from the amorphous boron and elemental magnesium during a 200 h ball milling under a hydrogen atmosphere [20]. After subtracting the contributions of the Scotch tape, the XRD profiles were used to calculate the average crystallite size (Table 2).

With respect to Table 2, firstly, it should be noted that the agglomeration and cold welding of the metal particulates to the reactor wall and the milling balls occurred during the milling process of the ductile magnesium under an inert gas. The gray line in Table 2 indicates that there is a severe agglomeration and cold welding of the powder particles to the stainless steel reactor wall. In such cases, the amount of the collected powder is so small that the experimental conditions should be ruled out despite the fact that the obtained particle size (or crystallite size) is small in some cases. Secondly, it was observed that the crystallite size and particle size do not coincide with each other at various experimental parameters. Experiment #1 (Mg–B 1111) presented the smallest particle size of 1.91 ± 1.61 μm. By contrast, the smallest crystallite size of 9.4 ± 1.1 nm was found in the experiment #7 (Mg–B 3132). To explore the effect of the nanostructure on hydrogen storage properties, both these experiments were chosen for further study.

Fig. 2 shows the typical SEM images of the powder of the smallest particle size (Mg–B 1111) and smallest crystallite size (Mg–B 3132). It can be seen that the particle size distribution ranges from a few micrometers to a dozen micrometers. In contrast to Mg–B 1111, the formation of the large particles in Mg–B 3132 is higher. The morphology of the particles demonstrates that the small hard boron particles were embedded into the soft magnesium particles.

3.2. Hydrogenation properties of the milled Mg–B powder

Soloveichik et al. reported that the onset decomposition temperatures of the low temperature and high temperature phases of $Mg(BH_4)_2$ are 285 and

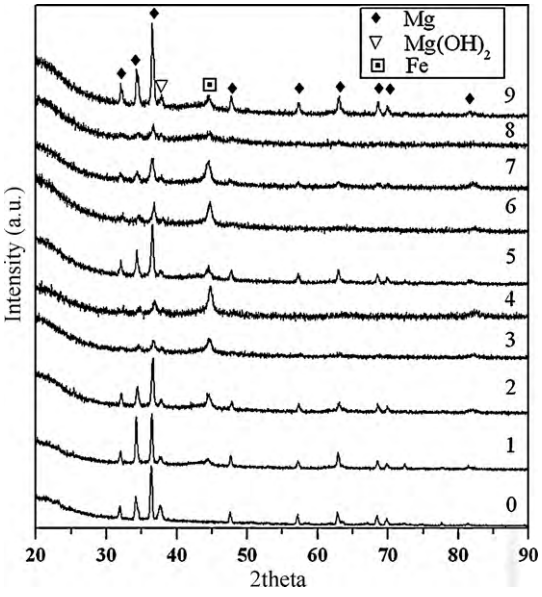

Fig. 1. XRD patterns of Mg–B powder milled under various milling parameters.

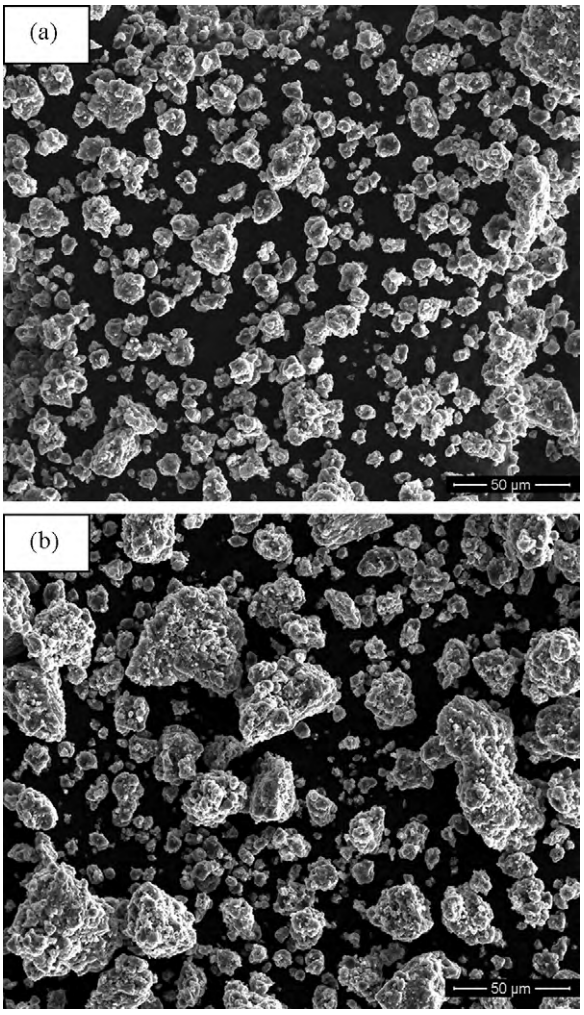

Fig. 2. Typical SEM images of the milled Mg–B powders: (a) Mg–B 1111 and (b) Mg–B 3132.

310 °C, respectively [9]. Therefore, in this study, the hydrogenation properties of Mg–B powders in a hydrogen atmosphere were examined at 300 °C using a pressure–composition–temperature (PCT) measurement. Fig. 3 shows the results for the powder of the smallest particle size (Mg–B 1111) and smallest crystallite size (Mg–B 3132). For Mg–B 1111, a plateau can be seen within the hydrogen pressure range of 0–3.8 MPa. The plateau pressure is approximately 2.2 MPa. The maximum absorbed capacity of hydrogen in this sample is 4.2 wt.%. In contrast to

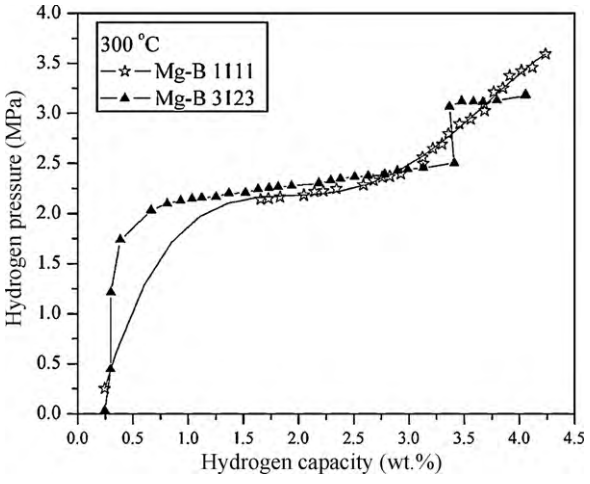

Fig. 3. PCT curves of the hydrogen absorption of Mg–B powder at 300 °C.

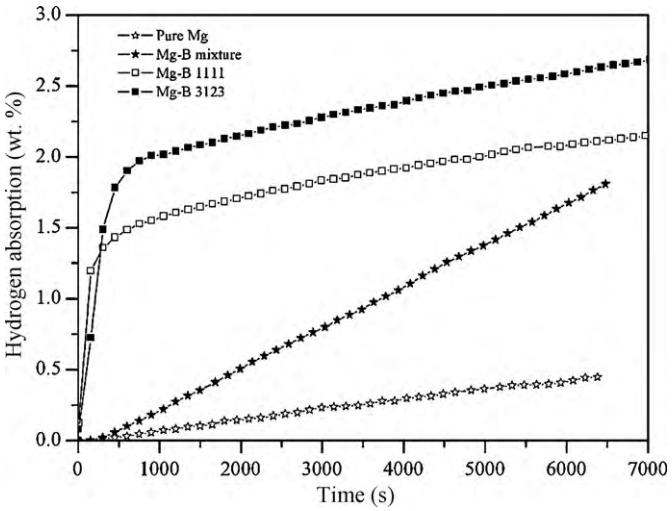

Fig. 4. Kinetic absorption curves of the pure magnesium, the unmilled mixture of magnesium and boron, the milled smallest particle size magnesium powder Mg–B 1111 and the milled smallest crystallite size Mg–B 3132, at 300 °C and 3 MPa hydrogen pressure.

Mg–B 1111, the hydrogen absorption curve of Mg–B 3132 demonstrates some difference regarding the two plateaus. The first plateau pressure is approximately 2.3 MPa, a little higher than that of Mg–B 1111. The second plateau pressure is approximately 3.0 MPa. In this case, the maximum absorbed capacity of hydrogen in the sample is 4.0 wt.%. The first plateau of both samples could be attributed to the formation of MgH_2 in contrast to the theoretical maximum absorbed hydrogen (4.1 wt.%) of the pure magnesium in the mixtures. Therefore, the second plateau of Mg–B 3132 is probably because of the formation of B–H intermediate compounds.

To compare the effects of the crystallite size and particle size on the absorption kinetic, kinetic curve measurements of Mg–B 1111 and Mg–B 3123 were carried out. Fig. 4 shows the obtained absorption kinetic curves at 300 °C with a hydrogen pressure of 3.0 MPa. As a reference, the kinetic curves of the unmilled pure Mg and the unmilled Mg–B mixture are also included. Fig. 4 shows that the hydrogenation process of the pure Mg is slow. Only 0.3 wt.% hydrogen is absorbed in nearly 7000 s because of the covered oxide layer on the Mg particle surface. However, the addition of B into Mg strongly accelerated the hydrogenation process. In this case, about 1.5 wt.% hydrogen was absorbed by the Mg–B mixture. Taking into account the compositions of this mixture (Mg:B = 1:2), the absorbed hydrogen in the magnesium could be approximately 3.0 wt.%. Therefore, it can be concluded that boron can strongly improve the absorption kinetics of magnesium hydrogenation. By contrast, it is well known that the ball milling process can also strongly improve the absorption kinetics of pure metals. It is not surprising that the milled powder showed much better absorption kinetics than the unmilled powders. Additionally, it is worth noting that the crystallite size showed a more obvious improvement of the absorption kinetic properties than that of the particle size when comparing the absorption curves of Mg–B 1111 and Mg–B 3123. The absorbed hydrogen concentrations of Mg–B 1111 and Mg–B 3132 in 7000 s were 1.8 and 2.5 wt.%, respectively.

3.3. Structural characteristics of the hydrogenated Mg–B powder

The XRD patterns of the obtained Mg–B hydrides after the kinetic measurements are shown in Fig. 5. It can be seen that for the pure Mg powder and the unmilled Mg–B mixture, the Mg phase is retained in the powder in addition to the impurities of $Mg(OH)_2$ and Fe, whereas the MgH_2 phase and B–H compounds are absent. Similar to the XRD patterns before hydrogenation, there is no evidence of the presence of the Mg(B) solid solution. By contrast, for the milled Mg–B 1111 and Mg–B 3132, most of the magnesium has transformed into MgH_2. In particular for Mg–B 3132, the Mg diffraction peaks can hardly be observed in the XRD pattern. However, in spite of the formation of MgH_2 in Mg–B 3132, the formation of B–H compounds cannot be identified from the XRD pattern. Therefore, a further examination of Raman spectra was carried out (Fig. 6). This demonstrated that there was no substantial difference in the Raman spectra among the original Mg–B mixture, the hydrogenation powder of the unmilled Mg–B mixture and the hydrogenation powder of Mg–B 1111. No B–H vibration mode can be observed for these samples. The band at approximately 750–1000 cm^{-1} is from the B–B vibration mode. For Mg–B 3132, a band at approximately 2500–2700 cm^{-1} appears, which suggests the formation of the B–H compound. This observed B–H vibration mode is consistent with the theoretical calculation as well as other experimental reports [10,11,21]. Therefore, a B–H intermediate compound possibly exists in the sample of Mg–B 3132. However, the quality of these compounds would be very small even if they are present in this sample. To further clarify the presence of the Mg–B–H compounds, TEM observa-

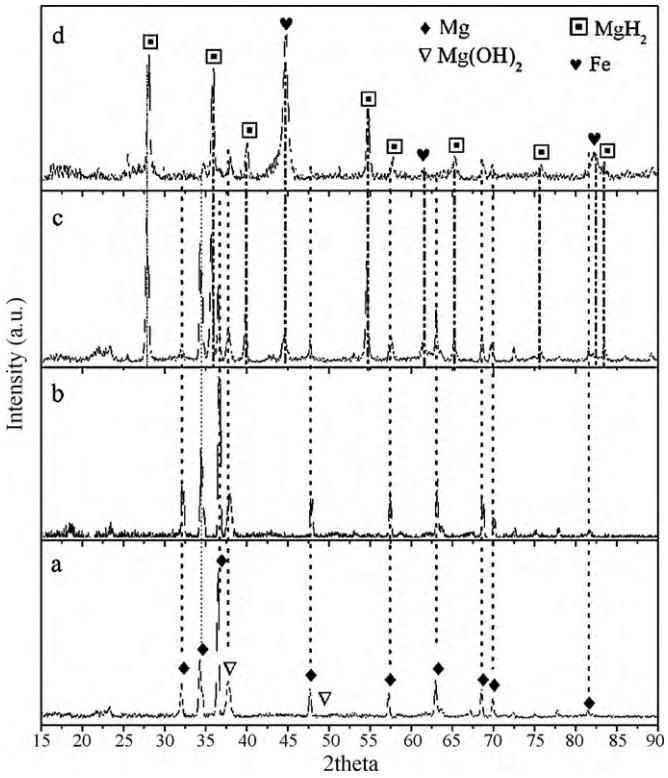

Fig. 5. XRD patterns of the milled Mg–B powder after hydrogenation: (a) original raw Mg–B mixture; (b) hydrogenation powder of Mg–B mixture; (c) hydrogenation powder of Mg–B 1111; and (d) hydrogenation powder of Mg–B 3123.

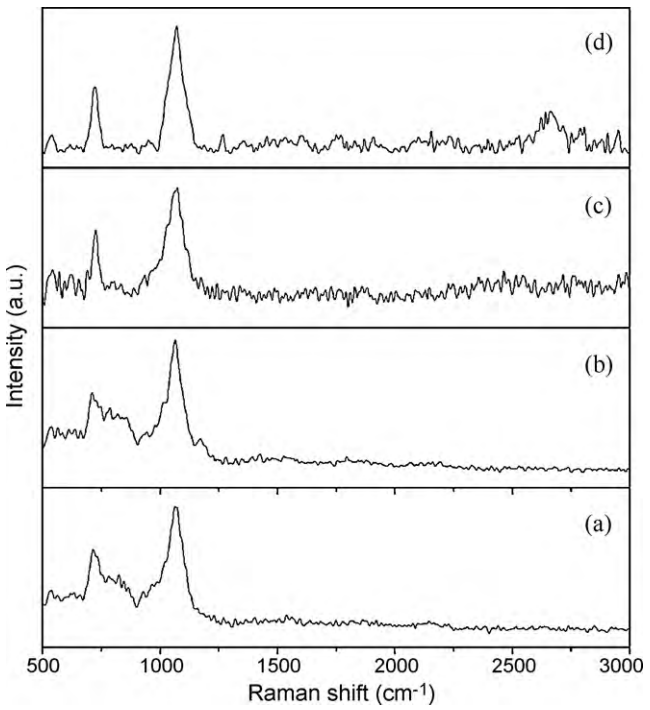

Fig. 6. Raman spectra of the milled Mg–B powder after hydrogenation: (a) original raw Mg–B mixture; (b) hydrogenation powder of Mg–B mixture; (c) hydrogenation powder of Mg–B 1111; and (d) hydrogenation powder of Mg–B 3123.

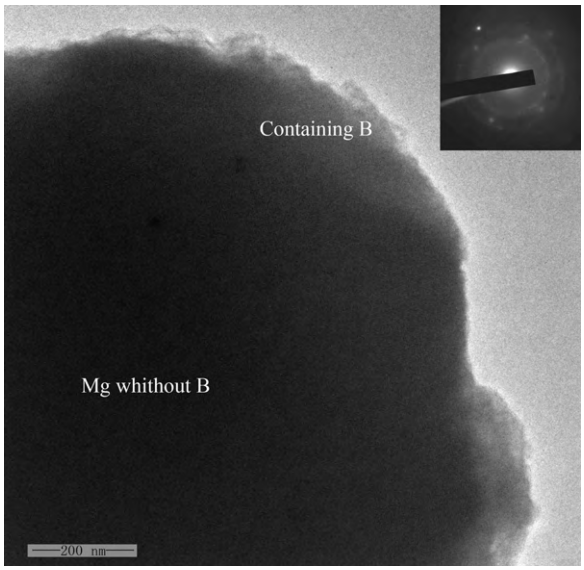

Fig. 7. TEM image and electron diffraction pattern of the smallest crystallite size Mg–B powder after hydrogenation.

tions were carried out. Fig. 7 shows the bright field image at the edge of a small particle and the corresponding diffraction image from the Mg–B 3132 hydride. The EDX test demonstrates that the distribution of B in the particles was not homogeneous; only at the edges of this image can the B element be found. In addition, the EDX test also presents some Fe signals, which is consistent with the XRD results. The diffraction pattern indicates that the particle consists of nanocrystalline and amorphous phases. The nanocrystalline phase can be attributed to MgH_2, whereas the amorphous phase probably corresponds to the boron phase.

4. Discussion

It has long been known that nanostructured materials have large surface areas, which facilitate the forming of more defects on the particle surface, the nucleating of the product phase heterogeneously, the shortening of the diffusion length of the constitutive elements and possibly the lowering of hydrogen reaction enthalpy [12]. Ball milling is an effective way to produce nanostructured powder. However, it should be noted that the ultimate crystallite size of a pure metal during milling is determined by the minimum grain size that can sustain a dislocation pile-up with a grain and by the rate of recovery during milling [22]. This ultimate crystallite size is an intrinsic property of the pure metal. For metal magnesium, the estimated ultimate crystallite size is 15 nm. However, in this study, the calculated crystallite size was a little smaller, which can be explained from the viewpoint of structural variation. It is assumed that a minute amount of boron element entered into the magnesium lattice and changed the lattice structure of the magnesium. However, since the amount of boron element and the atomic radius of boron are small the variations could hardly be detected in the XRD pattern. It has been reported that the formation of the MgB_2 phase can occur during a long-term milling under a hydrogen atmosphere [20]. However, in this study, there was no any evidence of the existence of the MgB_2 phase in any of the samples. The only obvious evidence was the presence of Fe from the milling balls (or the vial wall). This is inevitable during the ball milling process and might have affected the final hydrogenation properties of the Mg–B powders. Anyhow, further investigations on the effects of Fe on hydrogen storage properties are needed.

Our attempts to synthesize a ternary magnesium borohydride $Mg(BH_4)_2$ by mechanically milling the pure Mg and B powder and then hydrogenating under a hydrogen atmosphere did not succeed. This is in striking contrast to the successful mechanochemical synthesis of the nanostructured ternary complex hydride Mg_2FeH_6

[23]. However, it is similar to the unsuccessful attempt to synthesize alanates $Mg(AlH_4)_2$ [19]. The authors suggest that the formation of the Al(Mg) solid solution inhibited the reaction among MgH_2, Al and H_2. In this study, the failure cannot be attributed to the formation of the Mg(B) solid solution since there was no evidence of its presence. Moreover, the presence of $Mg(OH)_2$ had little effect on the hydrogenation properties since a further experiment to synthesize $Mg(BH_4)_2$ from highly pure magnesium and boron also failed. Additionally, it should be noted that it is difficult to avoid the occurrence of $Mg(OH)_2$ or MgO. The absence of hard oxides during ball milling under an inert atmosphere can aggravate the agglomeration or cold weld in our experience. There has been no successful reports of synthesizing magnesium borohydrides from pure boron, whether with Mg under a hydrogen atmosphere or with binary hydrides of MgH_2 directly. The most similar way of forming $Mg(BH_4)_2$ is the reversible reaction from dehydrated $Mg(BH_4)_2$ products [21]. It has been found that the formation of a $B_{12}H_{12}$ cluster instead of a $Mg(BH_4)_2$ hydride could be identified even under a very high hydrogen pressure of 40 MPa and a temperature of 400 °C for 48 h.

The reaction of B with the other elements is difficult at an ambient temperature and atmosphere. A high temperature and high pressure are usually needed to form B compounds because of the stronger atomic bonds of B–B. To form $Mg(BH_4)_2$, the B–B bonds in the icosahedral cluster of the amorphous boron need to be broken and the B atoms need to migrate to form $[BH_4]^-$. The barrier against breaking the B–B bonds and the migration of the B atoms is too high to be crossed under general conditions [21]. Therefore, it can be concluded that the formation enthalpy of $Mg(BH_4)_2$ from pure Mg, B and H_2 is more favorable than any other route from binary compounds. However, the synthesis is still hardly achieved because of the barriers against breaking the B–B atomic bonds and the migration of the B atoms. In contrast to the requirement to break the stronger B–B bonds, the formation of other B–H clusters such as $[B_{12}H_{12}]^{2-}$ requires less energy because the B–H cluster is similar to the icosahedral cluster in the amorphous boron [21]. In summary, a reversible hydrogen storage system in the borohydrides should be limited to a condition that the decomposition products do not involve the pure boron. In other words, the reversible process of the borohydrides should be between the metal borohydrides and the intermediate products including boron (i.e. MgB_2 or $[B_{12}H_{12}]^-$ containing products). This will undoubtedly reduce the attraction of metal borohydrides as a potential hydrogen storage material unless a catalyst facilitating the breaking of the atomic bond of B–B can be found.

5. Conclusion

A feasibility study of synthesizing magnesium borohydride $Mg(BH_4)_2$ by mechanically milling pure Mg and B powder following a hydrogenation process under a hydrogen atmosphere was carried out. Magnesium borohydride $Mg(BH_4)_2$ was not synthesized under these experimental conditions despite using optimized ball milling parameters, that is a smallest particle size of 2.64 μm and a smallest crystallite size of 9.4 nm. It was found that the addition of B into magnesium can strongly enhance the kinetic properties of magnesium hydrogenation. The reduction of crystallite size showed a more obvious effect on improving the absorption kinetic properties than that of the particle size. A possible B–H intermediate compound was found in the sample of Mg–B 3132 with a crystallite (particle) size of 9.4 nm (3.8 μm). The formation of $Mg(BH_4)_2$ from the pure elements was difficult because of the barriers against breaking the B–B atomic bonds and the migration of the B atoms. It is proposed that the reversible process of metal borohydrides should be between the metal borohydrides and the intermediate products including boron.

Acknowledgments

The financial support of the China Postdoctoral Science Foundation, the Foundation for Young Scientists of South China University of Technology, the Fundamental Research Funds for the Central Universities and the National Program on Key Basic Research Project (No. 2010CB631300) are gratefully acknowledged.

References

[1] S. Satyapal, J. Petrovic, C. Read, G. Thomas, G. Ordaz, U.S. The, Catal. Today 120 (2007) 246–256.
[2] T.K.M.a.D.H. Gregory, Annu. Rep. Prog. Chem. Sect. A: Inorg. Chem. 105 (2009) 21–54.
[3] S.-J. Hwang, R.C. Bowman Jr., J.W. Reiter, J. Rijssenbeek, G.L. Soloveichik, J.-C. Zhao, H. Kabbour, C.C. Ahn, J. Phys. Chem. C 112 (2008) 3164–3169.
[4] A.M. Seayad, D.M. Antonell, Adv. Mater. 16 (2004) 765–777.
[5] B. Sakintuna, F. Lamari-Darkrim, M. Hirscher, Int. J. Hydrogen Energy 32 (2007) 1121–1140.
[6] S.-I. Orimo, Y. Nakamori, J.R. Eliseo, A. Zuttel, C.M. Jensen, Chem. Rev. 107 (2007) 4111–4132.
[7] X.-F. Zhou, Q.-R. Qian, J. Zhou, B. Xu, Y. Tian, H.-T. Wang, Phys. Rev. B 79 (2009) 212102–212104.
[8] H.W. Li, K. Kikuchi, Y. Nakamori, K. Miwa, S. Towata, S. Orimo, Scr. Mater. 57 (2007) 679–682.
[9] G.L. Soloveichik, Y. Gao, J. Rijssenbeek, M. Andrus, S. Kniajanski, R.C. Bowman Jr., S.-J. Hwang, J.-C. Zhao, Int. J. Hydrogen Energy 34 (2009) 916–928.
[10] H.W. Li, K. Kikuchi, Y. Nakamori, N. Ohba, K. Miwa, S. Towata, S. Orimo, Acta Mater. 56 (2008) 1342–1347.
[11] R. Cerny, Y. Filinchuk, H. Hagemann, K. Yvon, Angew. Chem. Int. Ed. 46 (2007) 5765–5767.
[12] J. Yang, S. Hirano, Adv. Mater. 21 (2009) 3023–3028.
[13] P. Vajeeston, P. Ravindran, A. Kjekshus, H. Fjellvag, Appl. Phys. Lett. 89 (2006) 1906.
[14] V. Ozolins, E.H. Majzoub, C. Wolverton, Phys. Rev. Lett. 100 (2008).
[15] T. Matsunaga, F. Buchter, K. Miwa, S. Towata, S. Orimo, A. Zuttel, Renew. Energy 33 (2008) 193–196.
[16] G.L. Soloveichik, M. Andrus, Y. Gao, J.C. Zhao, S. Kniajanski, Int. J. Hydrogen Energy 34 (2009) 2144–2152.
[17] F.L. Zhang, M. Zhu, C.Y. Wang, Int. J. Refract. Metals Hard Mater. 26 (2008) 329–333.
[18] C.P. Balde, B.P.C. Hereijgers, J.H. Bitter, K.P. De Jong, J. Am. Chem. Soc. 130 (2008) 6761–6765.
[19] R.A. Varin, C. Chiu, T. Czujko, Z. Wronski, Nanotechnology 16 (2005) 2261–2274.
[20] Z. Wronski, R.A. Varin, C. Chiu, T. Czujko, A. Calka, J. Alloys Compd. 434/435 (2007) 743–746.
[21] H.W. Li, K. Miwa, N. Ohba, T. Fujita, T. Sato, Y. Yan, S. Towata, M.W. Chen, S. Orimo, Nanotechnology 20 (2009).
[22] J. Eckert, Nanostruct. Mater. 6 (1995) 413–416.
[23] R.A. Varin, S. Li, Z. Wronski, O. Morozova, T. Khomenko, J. Alloys Compd. 390 (2005) 282–296.